Diffuse Interfacial Regions Between O/W Microemulsions at Low Surfactant Concentration: Phase Diagram, Composition and Structure

Reprinted from The Journal of Physical Chemistry, 1987, *91*, 4536.

Diffuse Interfacial Regions between Oil/Water Microemulsions at Low Surfactant Concentration: Phase Diagram, Composition, and Structure Investigations

Cecilia M. C. Gambi,*† Liliane Léger,‡ and Christiane Taupin‡

Laboratoire de Physique de la Matière Condensée, Collège de France, 75231 Paris, Cedex 05, France
(Received: September 26, 1986)

A phase diagram investigation, by visual observation, has been performed at different temperatures on the system brine/toluene/1-butanol/SDS for a 6.5% NaCl salinity and for a very low SDS concentration (0.01–0.3% w/w). In the range 16–26 °C a new behavior is detected, characterized by the appearance of a diffuse interface, a few millimeters thick. The composition and the structure of a typical sample have been investigated in that domain, as a function of temperature, by index of refraction, gas chromatographic, turbidity, and quasi-elastic light scattering measurements. The sample is composed of an upper transparent region of the oily type and a lower turbid region of the oil/water (o/w) microemulsion type, separated by a sharp interface; the diffuse interface appears between two regions of different turbidity and composition of the lower aqueous domain. To interpret the nonuniformity of the aqueous domain a discussion is provided in terms of incomplete phase separation, critical type regime, sedimentation of polydisperse globules due to gravity, and globules aggregation. A detailed analysis of the composition profile allows to pinpoint a peculiar composition of the interfacial film with a much higher alcohol/SDS ratio than usual which could be the origin of the new behavior.

Introduction

A microemulsion, which is a fluid mixture of water (or brine) and hydrocarbon, stabilized by amphiphilic substances (surfactant and often a cosurfactant), can exist as a single phase or coexist with an excess of oil or an excess of water or both (respectively the Winsor IV, I, II, and III phases).[1] The very low values of the interfacial tension between the microemulsion phase and the phase(s) in excess ($\simeq 10^{-3}$ dyn/cm) of Winsor's microemulsions, along with their very large solubilization capability, account for the growing interest in theoretical investigations[2,3] and in technological applications.[4,5] A system composed of water, toluene, sodium dodecyl sulfate (SDS), and 1-butanol in suitable proportions, for which the salt concentration in water is increased, exhibits a phase transition Winsor I → III → II. The structure of the microemulsion changes from oil-in-water to water-in-oil through a bicontinuous system.[6–8] Generally the interfaces between the microemulsion and the phases in excess are flat by visual observation and appear sharp or diffuse for systems far or close to critical points, respectively, the thickness being always smaller than 1000 Å.[9]

Recently, a new behavior of the brine/toluene/1-butanol/SDS system has been reported in the very low SDS concentration range.[10] The sample studied was characterized by a diffuse interface, a few millimeters thick, which separates two regions of very different turbidity in the aqueous domain of the system; an upper oily transparent region coexists with this aqueous domain and is separated from it by a sharp interface. We have to emphasize that such a diffuse interface has no analogy (being several orders of magnitude thicker) with that of usual Winsor phases close to critical points. In ref 10, the composition and the structure of one sample have been investigated for one temperature and one composition. In the present paper we extend the investigation in order to delineate the domains of the phase diagram in which such a peculiar behavior takes place, and try to understand its origin. The phase diagram investigation by visual observation has been performed in the temperature range 12–30 °C, for a 6.5% NaCl salinity (NaCl/brine), a brine/toluene ratio $\simeq 2$, and a 1-butanol content in the range 1.9–2.7% and for very low SDS concentrations 0.006–0.6% (proportions given in w/w). The composition and the structure of the aqueous domain are deduced by index of refraction, gas chromatographic, turbidity and quasi-elastic light scattering (QELS) measurements for one composition (called S sample) in the temperature range 18–24 °C. To interpret the thermal evolution of the samples, a discussion is provided in terms of incomplete phase separation, critical regime, and sedimentation of dispersed oily globules induced by gravity.

Materials and Methods

Samples Preparation. Toluene is from SdS or Merck (uvasol), 1-butanol from SdS (puran) or Merck, sodium dodecyl sulfate (SDS) from Serlabo or Merck, and NaCl from Prolabo or Merck; the water is either tridistilled or taken from a Millipore Milli-Q system. Commerical products are used without further purification. No influence of the trade mark is observed. The composition of the samples for the phase diagram investigation is reported in the subsection Phase Diagram in the Results section; the samples were stabilized at every temperature investigated, at 0.1 °C. The S sample is composed of brine 65.74% (NaCl salinity 6.5%), toluene 31.90%, 1-butanol 2.30%, and SDS 0.04% (w/w). The sample cell is placed inside an oven stabilized at ±0.025 °C. The constancy of the temperature within the cell is tested by a thermocouple (vertical and horizontal temperature differences are smaller than 0.01 °C in the range 20–30 °C). Care is taken to avoid evaporation. Stabilization time of more than a week is always allowed for the sample in all the experiments.

Index of Refraction Investigation. The method employed is the combination of the minimum deviation method[11] and the laser beam deflection technique.[12,13] The sample cell is prismatic

* Permanent address: Department of Physics, L. E. Fermi 2, University of Florence, 50125-Florence, Italy (to whom correspondence should be addressed).
† CISM (of the M.P.I.) and GNSM (of the C.N.R.) groups.
‡ GRECO "Microemulsions" du C.N.R.S.

(1) Winsor, P. A. *Trans. Faraday Soc.* **1948**, *44*, 376.
(2) Borzi, C.; Lipowsky, R.; Widom, B. *Faraday Symp. Chem. Soc.* **1985**, *20*, 1.
(3) Widom, B. *J. Chem. Phys.* **1986**, *84*(*12*), 6943.
(4) *Surface Phenomena in Enhanced Oil Recovery*; Shah, D. O., Ed.; Plenum: 1981.
(5) *Macro and Microemulsions: Theory and Applications*; ACS Monograph No. 272; Shah, D. O., Ed.; American Chemical Society: Washington, DC, 1985.
(6) Scriven, L. E. In *Micellization, Solubilization and Microemulsions*; Mittal, K. L., Ed.; Plenum: New York, 1977; Vol. 2, p 77. *Nature* **1976**, *263*, 123.
(7) Auvray, L.; Cotton, J. P.; Ober, R.; Taupin, C. *J. Phys. Chem.* **1984**, *88*, 4586.
(8) Auvray, L.; Cotton, J. P.; Ober, R.; Taupin, C. *J. Phys.* (*Les Ulis, Fr.*) **1984**, *45*, 913. *Physica B* (*Amsterdam*) **1986**, *136B*, 281.
(9) Meunier, J.; Langevin, D. *J. Phys. Lett.* **1982**, *43*, L-185.
(10) Gambi, C. M. C.; Léger, L.; Taupin, C. *Europhys. Lett.* **1987**, *3*(*2*), 213.
(11) Born, M.; Wolf, E. In *Principles of Optics*; Pergamon: New York, 1980.
(12) Good, R. J.; Stromberg, R. R.; Patrick, R. L. *Technique of Surface and Colloid Chemistry and Physics*; Marcel Dekker: New York, Vol. 1, p 213.
(13) Giglio, M.; Vendramini, A. *Phys. Rev. Lett.* **1975**, *35*(*3*), 168.

0022-3654/87/2091-4536$01.50/0

(Hellma, ordinary glass, prism angle $\alpha = 45°$, 4 cm height). A He–Ne laser beam (Spectra-Physics, Model 196 with attenuator) is smoothly focused on the sample and collected on a far screen. A two-mirror beam steering system, mounted on a micropositioning device (Micro-Controle), allows to displace the beam in order to scan the sample vertically, with a spatial resolution of 100 μm. Using a liquid of known index of refraction (toluene, $n = 1.4968$ at $T = 20$ °C[14]), the optical quality of the cell was tested at the different heights (h). The resulting relative accuracy on n is of the order of 0.04%. Due to the presence of a vertical index of refraction gradient inside the sample, the beam is deflected along the vertical axis on the screen of a length $d(h)$ measured by a Schottky barrier photodiode (single axis position sensing of the type LSC from United Detector Technology Inc.). The vertical displacement resolution on the detector is 1/100 mm. For small deflections (d) on the screen and large distances (L) between the sample and the screen ($d \simeq 10^{-3}$ m and $L \simeq 2$ m), the index of refraction gradient is

$$|dn(h)/dh|_h = d(h)/sL \quad (1)$$

where s is the sample thickness. Refraction at the exit pupil has of course to be taken into account. The full index of refraction profile $n(h)$ is then obtained by a numerical integration of the gradient data, taking as a reference value for $h = 0$ the index of refraction, n_0, measured by the minimum deviation method just below the meniscus of the oil–microemulsion interface. The absolute accuracy on each $n(h)$ value is conditioned by the absolute accuracy on the n_0 determination, i.e., 0.04%; however, the relative accuracy along a single profile, due to the accuracy on the vertical deflection measurements, results in the order of 0.002% as evaluated on a homogeneous solution. Due to the weakness of the vertical gradients, no appreciable aberration of the beam is expected after transmission through the sample.

A calibration of the detector electrical signal in terms of vertical position has been performed on a sample (S0 sample) with a composition similar to that of the S-sample but without SDS. This sample displays two transparent phases, an upper oily phase and an aqueous lower phase, separated by a concave meniscus placed almost at the oil–microemulsion (o–m) interface height of the S sample. In Figure 1 the electrical signal on the detector output, as a function of height, is reported for a typical S sample aqueous domain, along with the calibration line obtained on the S0 sample lower phase (temperature $T = 20.10$ °C). The points just below the meniscus of the o–m interface, corresponding to vertical deflection toward ground, can be ascribed to a 0.02° inclination of the laser beam with respect to the interface (in fact, in this case the beam undergoes total internal reflection at the interface itself due to the difference of the index of refraction at the surface (1.35–1.49)); when such a misalignment occurred, the corresponding points of the plots were ignored as the accuracy of the alignments was less than 0.02°.

Gas Chromatography. Gas chromatographic analysis is performed on a Perkin Elmer 1 System, using 2-m columns with Carbowax 20M, on Chromasorb W.

Intensity Profile Measurements. Intensity data are recorded as a function of height during the same runs as the index of refraction measurements, using the Schottky barrier photodiode signal which is proportional to the intensity of the spot falling on it. For a given spot position, the dark intensity is subtracted from the actual detected intensity; the precision of the single measurement is 1%. A calibration is made with the cell filled with pure toluene; when h is varied, the resulting accuracy decreases to 3% due to imperfections of the cell walls which scatters light. On the S0 sample lower phase the transmitted intensity is observed to be constant as a function of h; the values are distributed in the range 0.120–0.160 au at $T = 20.15$ °C. Fluctuations of the laser beam are low enough and do not affect significantly the results. The light energy is not absorbed, and thus transmittance is a measurement of the scattering ability of the sample.[15] Actually,

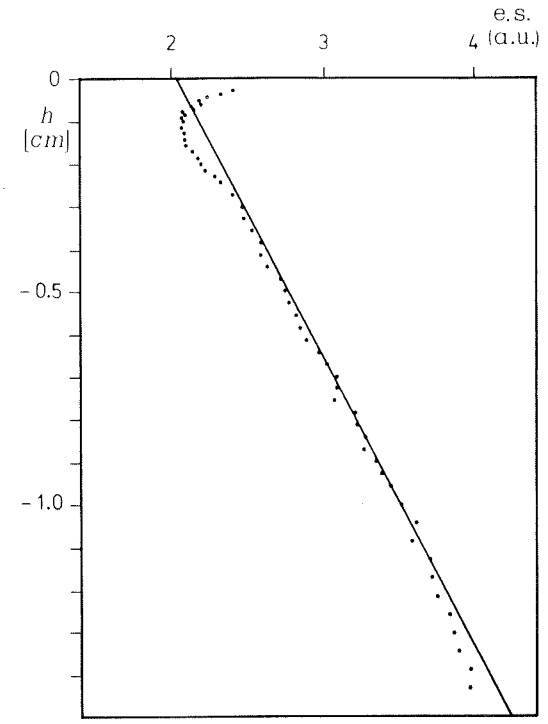

Figure 1. Index of refraction measurements. The experimental points correspond to the electric signals detected by the photodiode (vertical position of the beam) as a function of height inside the aqueous domain. The oil–microemulsion (o–m) interface is at $h = 0$ cm (just below the meniscus); the lower boundary of the sample is at $h = -1.75$ cm. The straight line is the calibration line evaluated with a linear regression from measurements on the S0 sample lower phase (the experimental points relative to the S0 sample are not reported in the picture). Temperature of the experiment, $T = 20.10$ °C. About ten points below the meniscus of the o–m interface are eliminated for the evaluation of the corresponding $n(h)$ profile (see curve b of Figure 5) for reasons which are detailed in the test.

the sample does not appear turbid (sample thickness is kept small, ≃3 mm), there is no diffuse zone around the laser spot on the screen, and multiple scattering is unlikely.

Quasi-Elastic Light Scattering Analysis (QELS). Dust-free samples are obtained by filtration through a Millipore microporous filter (0.2 μm pore size). Two different procedures are used: (a) every liquid component is filtered before mixing and then SDS is added; (b) the brine/1-butanol/SDS compound is prepared and then filtered before mixing with separately filtered toluene. In the second case, due to the small quantity of SDS used, in order to recover the desired SDS proportion in the filtered compound, care must be taken to saturate the filter in advance by filtering a large volume of the solution. No difference in the results is detected between samples prepared following the procedures a and b. The light source is a krypton ion laser (Coherent Radiation CR 500K, $\lambda = 530.9$ nm) suitably attenuated. Two cells are used: a sealed cylindrical cell (diameter 4 mm) and a Hellma square cell (ordinary glass, sample thickness 3 mm). A lens focuses the beam on the sample and another lens images the scattering volume on the entry pinhole of a photomultiplier. Both the focusing lens and the pinhole are chosen to ensure detection on one coherence area.[16] The photomultiplier is connected to a discriminator amplifier working in the photon counting mode and then to a digital correlator[17] with 100 channels (time resolution 0.5 μs). The practical resolution of the apparatus is 1 μs. The collecting arm can be rotated to adjust the scattering angle with a resolution of ±0.1°, in the range 0°–130°. A two-mirror beam steering system

(14) Timmermans *Physico-Chemical Constants of Pure Organic Compounds*; Elsevier: New York, 1965; Vol. 1, 2.

(15) Berne, B. J.; Pecora, R. *Dynamic Light Scattering*; Wiley: New York, 1976.

(16) Degiorgio, V. In *Photon Correlation Spectroscopy and Velocimetry*; Cummins, H. Z.; Pike, E. R., Eds.; Plenum: New York, 1976; p 142.

(17) Corti, M. In *Coherant Optical Engineering*; Arecchi, F. T.; Degiorgio, V., Eds.; North-Holland: Amsterdam, 1977; p 245.

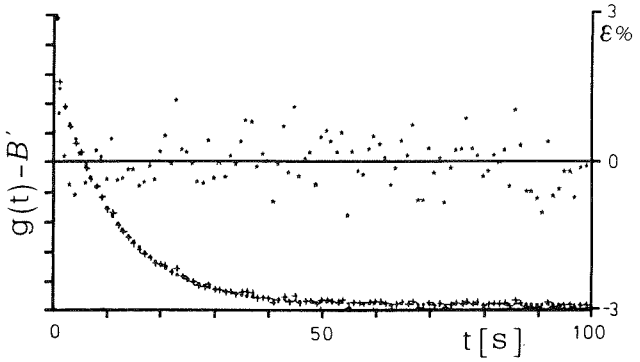

Figure 2. Typical plot of the correlation function of the scattered intensity vs. time. The points are relative to the best-fitted curve, $g(t) = A' \exp(-t/\tau) + B'$, to the experimental values (plus). The deviation ϵ between experimental and calculated values is also reported (stars).

is again used to vertically displace the beam. Correspondingly the collecting lens and the photomultiplier are vertically displaced to collect the signal at the different heights. Dynamic and static contributions, arising respectively from index of refraction fluctuations in the sample cell and static scatterers (cell walls), are detected. For fluctuations characterized by a single relaxation process, the correlation function of the phototube output results a single exponential only in the two limiting cases of homodyne and heterodyne regimes.[15,18] A typical correlation function vs. time curve is shown in Figure 2 along with the deviation ϵ between experimental data points and calculated curve. The adjustments were usually performed on 100 points covering more than four time constants of the exponential, and the experiments retained correspond to a quality factor $Q = 1 - \sum_{i=1}^{N-1} \epsilon_i \epsilon_{i+1} / \sum_{i=1}^{N} \epsilon_i^2$ better than 0.90 and to a χ^2 value smaller than 1.20 corresponding to an ϵ deviation 1.5% (homodyne detection). Due to the quality of the fit and to the signal-to-noise ratio, the exponential time constants are obtained with a relative uncertainty better than 3%.

To test the apparatus, a calibration procedure has been carried out on a dilute suspension of polystyrene spheres for different heights. In that case the scattering process is diffusive and the mutual diffusion coefficient of the particles, in homodyne detection is

$$D = 1/(2\mathbf{q}^2\tau) \qquad (2)$$

where $\mathbf{q}$ is the scattering wave vector ($=4\pi n \sin(\theta/2)/\lambda$, with n the index of refraction of the suspension and θ the scattering angle). The hydrodynamic radius of the particles can then be deduced by using the Stokes–Einstein formula.[15] We have checked that the measured value of the hydrodynamic radius is in good agreement with the nominal value (R_H = 518 Å) and remained constant at the different heights, within ΔR_H = 8 Å.

Results

Phase Diagram. A phase diagram investigation has been performed by visual observation of samples of varying composition in a SDS concentration range well below what usually leads to conventional Winsor phases. For all the following, the component proportions are given in percent, w/w; NaCl salinity 6.5%. The results are summarized on Figures 3 and 4.

First, in Figure 3 the ratio brine/toluene is kept constant (=2.02); the SDS is varied from 0.6% to 0.006%, covering the domain for which the new behavior has been observed.[10] The 1-butanol proportion is 2.52% for the five samples on the left and 2.3% for the others. The (a) and (b) series correspond respectively to T = 30 °C and T = 20 °C. For all the compositions, we have at least two regions. The upper transparent region appears identical throughout the samples (same volume). On the contrary, the lower part of the sample has an aspect which strongly depends on the SDS content, and one goes from a homogeneous micro-

(18) Benedek, G. B. *Optical Mixing Spectroscopy, with Applications to Problems in Physics, Chemistry, Biology and Engineering*, Presses Universitaire de France: Paris, 1969.

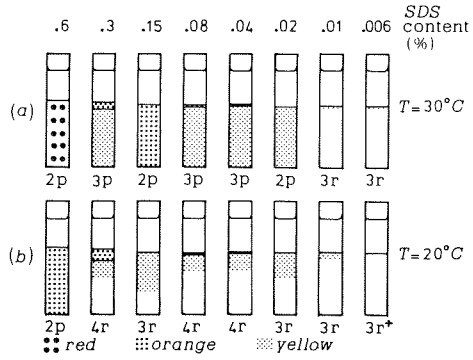

Figure 3. Schematic representation of the aspect of samples at two different temperatures (a and b sequences) for which the ratio brine/toluene is kept constant (2.02); the SDS is varied in the range 0.6–0.006% and the 1-butanol is 2.52% for the five samples on the left and 2.30% for the others. Differences in turbidity are manifested by different dot sizes.

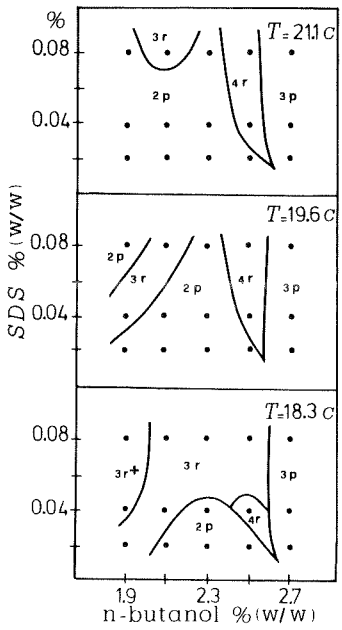

Figure 4. Schematic phase diagram of samples composed of brine (65.74%), toluene (31.90%), and SDS and 1-butanol varying in the ranges 0.02–0.08% and 1.9–2.7%, respectively, at three different temperatures. The points represent the compositions of the actually examined samples. The continuous lines are only guides for eye drawn to separate the different phase domains.

emulsion-type phase occupying the whole lower part (large SDS content) to a homogeneous transparent phase (low SDS content), through inhomogeneous systems. On the figure, we have represented the relative volumes of each region and distinguished transparent (colorless) and turbid phases. The latter ones appear blue in reflected light and red-yellow in transmission, if a white light source is used. The difference in the transmitted light color is pointed out in the picture. The color (wavelength) gives an approximate idea of the correlation length of the density fluctuations inside the samples, being larger for red than for yellow; the difference in opacity of the samples is not reported. Sharp interfaces are continuous lines; diffuse regions a few millimeters thick are undefined lines. Samples without diffuseness are called 2p and 3p for two- and three-phase equilibria, respectively; the 2p equilibrium is of Winsor I type. The other samples are called $3r^+$, 3r, and 4r samples, the different regions (separated by sharp or diffuse interfaces) being three and four, respectively; the $3r^+$ sample has two transparent regions, aqueous and oily, but a white structure spreads at the oily-aqueous sharp interface.

In Figure 4, complementary results are gathered: still keeping constant brine and toluene content, the SDS and 1-butanol compositions have been varied respectively in the ranges 0.02–0.08% and 1.9–2.7%. Fifteen samples of different compositions (dots

on the figure) have been visually investigated for three different temperatures (T) stabilized at 0.1 °C. The lines are only guides to fix the limits between different regions of the phase diagram. The temperature increase does not change the 3p equilibrium; however, it extinguishes the $3r^+$ region, floods the 2p and 4r regions, and displaces the 3r region to higher surfactant concentration. For the compositions investigated, an alcohol increase always leads to a 3p equilibrium. For the samples of Figures 3 and 4, no diffuse region is displayed below 16 °C and above 26 °C; for $T < 16$ °C the surfactant spreads on the oil–microemulsion (o–m) interface and on the cell walls and no microemulsion feature is shown. The $3r^+$ equilibrium in which the surfactant spreads on the interface without spreading on the cell walls is an intermediate case between the low-temperature behavior just described and the room temperature behavior (2p or 3r cases). For the 3r-type samples, removing the upper oily phase does not affect the aqueous domain.

In summary, the phase diagram observations suggest that, for the brine/toluene ratio $\simeq 2$ at the salinity 6.5%, the temperature range in which the diffuseness of the aqueous domain exists is ~16–26 °C, the upper SDS value being 0.3% and the lower one 0.006%; the 1-butanol content is within 1.9 and 2.5% approximately. Thus the SDS/1-butanol ratio for samples displaying diffuseness results less than ~0.1 for 4r samples and less than ~0.06 for 3r samples. The results of the low-temperature observation suggest that the SDS content is likely close to its solubilization limit for the given proportion brine/toluene $\simeq 2$ and the given 1-butanol content at the salinity of 6.5%.

We have to point out that the phase diagram shown in Figures 3 and 4 is only a small segment of the general phase diagram of the brine/toluene/1-butanol/SDS microemulsion system. Bellocq et al.[19] have presented a much more extended study of the phase diagram of this system but not in the very low SDS concentration range we study here. It is interesting how our observations link those of ref 19. In Figure 9 of ref 19, the developing of a Winsor III equilibrium is shown at a 6% NaCl salinity vs. the increase of the 1-butanol/SDS ratio within 0.9 (phase diagram a) and 9 (phase diagram f). One of the main results of ref 19 is that, due to the increase of the alcohol/surfactant ratio, the percentage of the active mixture necessary to obtain a Winsor III equilibrium decreases and the shape of the Winsor III region lengthens along the water–oil edge of the tetrahedron and is quite narrow in the surfactant–alcohol direction. The slightly higher salinity value used in our case, 6.5%, should not drastically change the phase diagram; in fact, from the observation of phase diagram e of ref 19, the sample on the left of Figure 3 (this paper), for which the alcohol/SDS ratio is ~4, is expected to be a Winsor I equilibrium and the second sample from the left of the same figure (alcohol/SDS ~ 8), a Winsor III one. Indeed for Winsor I equilibrium, the correspondence is exactly verified. For the Winsor III equilibrium this is not the case. In general, should the trend described in ref 19 be valid also for higher alcohol/SDS ratios than those tested there, we could expect Winsor III equilibria for all the samples of Figure 3 except the first on the left (active mixture percentage in the range 2.8–2.3%). Furthermore, a Winsor III equilibrium should be displayed by the samples of Figure 4, for which an active mixture percentage down to 1.9 has been analyzed. On the contrary, samples with diffuse aqueous domains are shown.

Index of Refraction. The S-sample phase compositions as well as the composition profile inside the aqueous domain have been evaluated from the index of refraction measurements. When displacing the beam vertically through the S sample we observe (1) no n variation in the upper region which is thus assumed to be uniform in composition, and (2) below the sharp o–m interface, an index of refraction profile indicating a progressive variation of the composition. The measured upper region index of refraction value (n_u) is reported in Table I for the different temperatures investigated along with the measured n values of the S0 sample

TABLE I: Index of Refraction of S0 and S Sample Phases and of the Mixture Components at Different Temperatures in the Investigated Temperature Range

	T, °C	n	ρ, g/mL	MW
S sample				
upper phase	18.15	1.4943		
upper phase	20.10	1.4930		
upper phase	24.20	1.4905		
S0 sample				
upper phase	20.15	1.4933		
lower phase	20.15	1.3480		
toluene	18	1.4980	0.868 78	92.14
	20	1.4968	0.866 90	92.14
	24	1.4946	0.863 14	92.14
1-butanol	18	1.3999	0.811 11	74.12
	20	1.3991	0.809 61	74.12
	24	1.3974	0.806 46	74.12
brine (6.5 wt % of NaCl)	20	1.3444	1.044 95	18.85
SDS	20	1.46	1.16	288

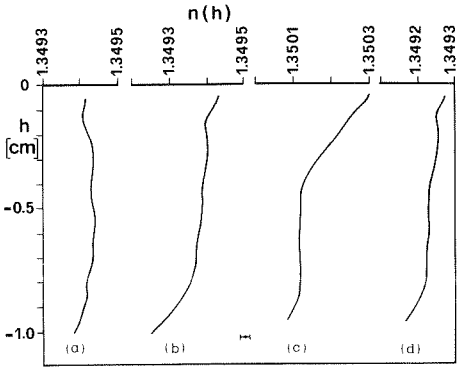

Figure 5. $n(h)$ profiles for the aqueous domain at different temperatures. The o–m interface is at $h = 0$ cm; the lower boundary of the sample is at $h = -1.75$ cm (for $h < -1.0$ cm the investigation was not possible because of the walls of the oven). Temperature of the experiments: (a) 18.15 °C; (b) 20.10 °C; (c) 22.15 °C; (d) 24.20 °C. The error bar represents the relative indetermination along the profile.

upper and lower phases at $T = 20$ °C and the n value, the density value plus the molecular weight (MW) of the mixture components as found in the literature.[14,20,21] In Figure 5 the $n(h)$ profiles (with h = distance to the o–m interface) are given, at four different temperatures (18.15, 20.10, 22.15, and 24.20 °C), for the aqueous domain of the S sample. $h = 0$ cm corresponds to the first measurable point just below the meniscus of the o–m interface for all the profiles presented. The relative error bar (0.002%) is shown in the picture. From the observation of the profiles, three regions can be identified: (a) a subinterface region with linear n variation immediately below the meniscus of the o–m interface (not identified by the visual observation of the phase diagram investigation); (b) an intermediate region with a constant n value; (c) a region with rapidly varying n (for $-0.5 \geq h \geq -1.0$ cm) corresponding to the diffuse region. The investigation was not possible for $h < -1$ cm due to the presence of the oven walls whose window's size was the result of a compromise: minimization of thermal gradients and efficiency in the profile detection. Except eventually for a small subinterface region of the (a) curve, the n value decreases from the o–m interface to the bottom of the sample for all the temperatures. The curves a and d of Figure 5 display $n(h)$ variations smaller than those of the curves b and c. This fact suggests that, for $T < 18$ °C and $T > 24$ °C, the whole aqueous domain becomes homogeneous, and confirms the visual observation reported in the subsection Phase Diagram; the 3r regime becomes a $3r^+$ at lower temperatures and a 2p equilibrium at higher temperatures. Curves b and c of Figure 5 display important $n(h)$ variations, the stronger variation being for $-0.5 \geq h \geq -1.0$ cm in curve b ($T = 20$ °C) and for $0 \geq h \geq -0.5$ cm

(19) Bellocq, A. M.; Biais, J.; Clin, B.; Gelot, A.; Lalanne, P.; Lemanceau, B. *J. Colloid Interface Sci.* **1980**, *74*(2), 311.

(20) *Handbook of Chemistry and Physics*, 51st ed.; The Chemical Rubber Co.: Boca Raton, FL, 1970–1971.

(21) Reiss-Husson, F.; Luzzati, V. *J. Phys. Chem.* **1964**, *68*, 3504.

TABLE II: Phase Compositions As Evaluated by the Measured Index of Refraction Values, at T = 20 °C, for the S0 Sample and at T = 18, 20, and 24 °C for the S Sample

	tot composn of the samples, mL		vol of the components for each phase, mL					
			S0 sample		S sample			
	S0	S	upper phase	lower phase	aqueous domain	upper phase	upper phase	upper phase
temp, °C			20	20	20	20	24	18
n value of the phase			1.4933	1.3480	1.3490	1.4930	1.4905	1.4943
toluene	0.58	0.58	0.5630	0.0167	0.0234	0.5566	0.5590	0.5554
1-butanol	0.045	0.045	0.0202	0.0248	0.0248	0.0202	0.0203	0.0202
brine (6.5% salinity)	1.00	1.00		1.00	1.00			
SDS		5.81×10^{-4}			5.81×10^{-4}			

in curve c (T = 22 °C) (subinterface region at that temperature).

In order to transpose the index of refraction measurements in terms of composition, several hypotheses are needed that we shall now detail. All the analysis has been done using the S0 sample as a reference. Analysis of the S0 sample: A priori we have three components (toluene, brine, and 1-butanol) which can part between the two phases. We are left with three unknown (the three partition coefficients) while we have two measurements (the two index of refraction of upper and lower phases). In order to evaluate the compositions, we have assumed that there was no water in the upper phase. Using the refractivity formula[11] we can deduce the compositions of the two phases at 20 °C (they are reported in Table II); we see that the 1-butanol parts almost in equal quantities into the two phases. A more surprising result is the rather large amount of toluene present in the lower aqueous phase. We attribute this behavior to the larger solubilization capability of 1-butanol in toluene than in water, in agreement with the water–butanol–toluene phase diagram.[22] We have to assume that the salt does not affect the oily phase composition.[23,24] These results are not affected if we introduce the finite solubilization limit of toluene in water and vice versa (0.045% w/w, identical in the two cases[25]) which gives a negligible correction. Analysis of the S sample: The total composition of the S sample differs from the S0 sample only for the SDS addition. The n_u values at three different temperatures and the average n value of the S sample aqueous domain at T = 20 °C are reported in Table II. The values obtained for T = 20 °C can be compared to the corresponding values of the S0 sample. First the n_u values are identical within experimental error; on the contrary, the n value of the S sample aqueous domain is larger than the n value of the S0 sample lower phase. We interpret that fact by assuming that, due to the SDS, more toluene is transferred from the upper region to the aqueous domain (the addition of all the SDS does not justify the observed n value of this last). The quantity of transferred toluene can be evaluated by the refractivity formula assuming that all the SDS is in the aqueous domain; it leads to the composition reported in Table II. For the upper region, the composition obtained by subtraction to the total composition is also reported in Table II. The calculated n_u value (1.4932), agrees with the measured value (1.4930) within the experimental error (±0.0003). This fact supports the validity of the hypotheses used to calculate the composition.

A test on the composition variation vs. the temperature can be done using the n_u values detected at the different temperatures (see Table I); within the experimental error, there is no difference between the n average values (or maximum values) of the aqueous domain at the different temperatures; however, the difference between the n values of the upper region is larger than the experimental error. Starting from the upper region composition of the S sample at T = 20 °C, we can calculate the corresponding

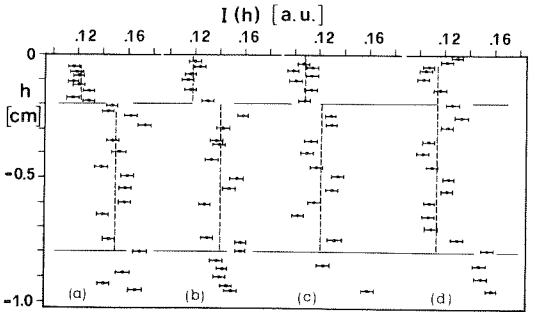

Figure 6. $I(h)$ profiles detected in the same conditions as for the $n(h)$ profiles. The horizontal full lines delimit the subinterface (0 cm ≥ h ≥ −0.2 cm) and the intermediate (−0.2 cm ≥ h ≥ −0.8 cm) regions. The dotted lines single out the average value of the region.

toluene and 1-butanol volumes at T = 24 °C and T = 18 °C (the values are reported in Table II). The evaluated n values are 1.4911 and 1.4945; they correspond to the measured values (1.4905 and 1.4943, respectively) inside the experimental errors. This fact could suggest that, in the range 18–24 °C, the upper region composition, in weight, remains unchanged; in that case the aqueous domain average composition should remain the same, by weight, in the same thermal range. This fact agrees with the observation that taking away the upper region does not imply macroscopically any change in the aqueous domain; the intermediate and lower regions remain separated by the diffuse region, also if the aqueous domain, separated from the upper oily region, is shaken and newly stabilized. In principle, however, we cannot exclude a different distribution of the components between the upper oily region and the aqueous domain at the different temperatures investigated.

The n profile inside the intermediate and lower regions of the aqueous domain implies a composition distribution; we postpone its evaluation after the presentation of the other results.

Gas Chromatography. A gas chromatographic investigation has been done to characterize more precisely the compositions of the S and S0 samples upper regions at T = 20 °C.[10] We just summarize here the results: the 1-butanol/toluene ratios result in 2.44% and 1.46% for S and S0, respectively. This implies that the SDS addition to the mixture transfers toluene from the upper region to the aqueous domain in good agreement with the evaluation of the S-sample composition derived from the index of refraction measurements.

Transmitted Intensity. In Figure 6 the intensity transmitted through the S sample, I, is given at four different temperatures as a function of height inside the aqueous domain. Besides the large uncertainty of the data points, general trends can be noticed. The scattering power of the aqueous domain is not uniform. After a zone of strong scattering located just below the o–m interface, for 0 cm ≥ h ≥ −0.2 cm, an intermediate region with approximately constant scattering power appears (−0.2 cm ≥ h ≥ −0.8 cm) eventually followed by a less scattering zone (see Figure 6, c and d). When the temperature is varied, the whole $I(h)$ profile is deformed: the strongly scattering subinterface region progressively disappears when T increases from 18 to 24 °C, while the I value in the intermediate region slowly decreases. For comparison, measurements performed at 20.15 °C on the S0

(22) Ho, P. C.; Kraus, K. A. *J. Colloid Interface Sci.* **1979**, *70*, 537.
(23) Biais, J.; Clin, B.; Lalanne, P.; Barthe, M. In *Surfactants in Solution*; Mittal, K. L.; Lindman, B. Eds.; Plenum: New York, 1984; p 1789.
(24) Roux, D.; Bellocq, A. M.; Leblanc, M. S. *Chem. Phys. Lett.* **1983**, *94*(2), 156.
(25) Stephen, H.; Stephen, T. *Solubilities of Inorganic and Organic Compounds*; Section Binary System, vol. 1 and 2; Van Nostrand: New York, 1952.

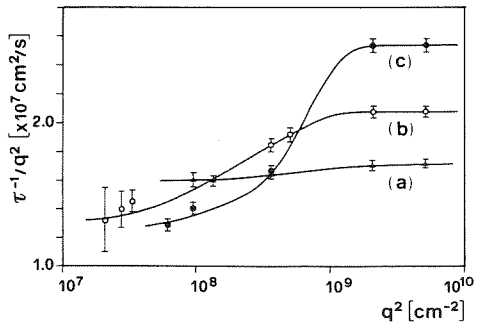

Figure 7. τ^{-1}/q^2 dependence vs. q^2 (angular range 9–90°) for three different heights: (a) intermediate region (triangle); (b) diffuse region (circles); (c) lower region (full circles). Temperature of the experiments T = 20.34 °C. The lines are guide for the eyes. τ values are obtained assuming homodyne detection. The observed decrease can be attributed to a progressive transition toward heterodyne detection at small scattering angles.

sample display a uniform $I(h)$ curve around the value 0.14, the span of the distribution being the same as for the lower part of the S-sample profile ($h < -0.2$ cm) at the same temperature (curve b). Thus, presence of the surfactant does not change the I value of the bottom part of the sample, in the resolution limit of the detector, while it leads to a strong scattering in the subinterface region. Comparing Figures 5 and 6, we see that for all the temperatures tested, the general trends are in correspondence: the $I(h)$ increase toward the bottom of the cell parallels the $n(h)$ decrease, i.e., the oil percentage decreases. This suggests that the scattering power of the sample can be attributed to a dispersion of oily globules throughout the aqueous domain. However, a more careful examination of Figures 5 and 6 reveals differences between the $n(h)$ and $I(h)$ behavior, especially in the subinterface region for curves *a* and *c*. For the curve a this can be an experimental artifact: at this temperature (T = 18 °C) the surfactant is very close to its solubility limit and tends to deposit on the cell walls, especially close to the o–m interface; this could subtract a part of the transmitted intensity without changing significantly the n properties of the region. For curve c the $n(h)$ profile in the subinterface region appears different from all the other curves and could indicate that the stabilization of the sample was not exactly reached for that particular experiment as will be discussed in the subsection Stabilization of the Samples.

QELS Analysis. The autocorrelation function of the scattered intensity $g(t)$ has been measured as a function of height all throughout the S sample. In the upper region no relaxation time of $g(t)$ is detectable in the limit of resolution of the apparatus. This implies that no aggregates of supramolecular size are present there, in good agreement with the index of refraction data. In the aqueous domain, on the contrary, we do detect a correlation time for all the investigated heights down to the bottom of the cell. For each h value the q dependence of that correlation time has been characterized and typical results, assuming homodyne detection, are gathered in Figure 7 for three different heights belonging to the intermediate (a), diffuse (b), and lower (c) regions. For a diffusive process, τ^{-1}/q^2 has to be independent of q^2. The observed decrease when going to small q values can however be explained in terms of a transition from homodyne to heterodyne detection, for θ values somewhere between 90° and 0°. Heterodyne is due to a static field (local oscillator) essentially scattered in the forward direction, because of the n mismatch at the interior cell walls. Depending on the intensity of the signal, the angular range at which one goes from pure homodyne to pure heterodyne detection varies and is displaced toward larger q values for a larger signal. Due to the intensity variation of the aqueous domain, the trends of Figure 7 seem likely explained by such a change in detection regime. Moreover, a complete transition from homodyne to heterodyne leads to a decrease by a factor 2 of the apparent τ^{-1}/q^2 value as observed on curve c for which the scattered signal is the smallest (lower region). For curves b and a, the local oscillator is not sufficient to fully heterodyne the large

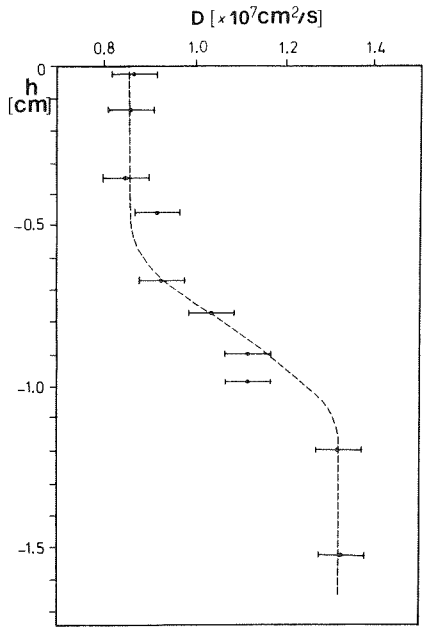

Figure 8. Mutual diffusion coefficient vs. the height, detected at θ = 90° for the aqueous domain of S sample; temperature of the experiments T = 20.34 °C. The o–m interface is placed at h = 0 cm and the bottom of the sample at h = −1.75 cm. The dotted line is a guide for the eyes. Three zones are in evidence: intermediate and lower regions at constant D value (differing by a factor 1.5) and a diffuse region with a progressive variation from one constant value to the other.

scattered signal even at low scattering angles ($\theta \geq 6°$). The scattered field due to the cell walls–air interface is suppressed by imaging it outside the input pupil of the photomultiplier. In any cases, constant τ^{-1}/q^2 values are detected between 45° and 90° at the different heights; this implies that pure homodyne detection is indeed obtained for θ = 90°, characterized by eq 2.

The $D(h)$ dependence for the aqueous domain of the S sample is reported in Figure 8 (T = 20.34 °C). The profile is the result of two different experimental runs on the intermediate plus diffuse regions and on the diffuse plus lower regions; the last is done after vertical displacement of the cell to avoid the oven's walls. We waited the time necessary to obtain D values of the intermediate region identical in the two cases. In contrast to the $n(h)$ and $I(h)$ detection, the good absolute accuracy of the D measurement makes it possible to follow this procedure in order to detect the D values throughout the aqueous domain. Two regions of constant D value appear for $0 \leq h \leq -0.5$ cm (intermediate) and $-1.2 \leq h \leq -1.6$ cm (lower), respectively, separated by a region of rapidly varying D value (diffuse). Measurements have also been conducted for an S sample in the prismatic cell and in a cylindrical cell, and lead to the same results inside the experimental errors, implying that the cell geometry is not important. A temperature exploration has been performed at T = 23.78 °C. The D values obtained at three different heights from −0.05 to −0.70 cm coincide with those reported in Figure 8 within the experimental errors, indicating a $D(h)$ dependence of the intermediate region independent of T in the range 20–24 °C. At T = 23.78 °C the $\tau^{-1}/q^2(q^2)$ dependence has also been tested for h = −0.7 cm (diffuse region). In the angular range investigated (15°–90°), the τ^{-1}/q^2 values are constant, implying that the detection is homodyne for all the angles tested. This fact suggests that an increase in temperature increases the scattered power of the diffuse region (thus homodyne detection becomes possible for all the angles investigated in that region). We have to point out that the subinterface region has not been detected in terms of a $D(h)$ change at θ = 90°. This may not be contradictory and implies the presence of large scattering globules which strongly contribute to the scattering in the forward direction but are not detectable in the dynamic experiment performed at large angle.

Stabilization of the Samples. One important question is of course to know if the sample represents a real thermodynamic

stable state. This is indeed a very difficult question. To try to elucidate that point, we have followed the time evolution of the $n(h)$ and $I(h)$ profiles after shaking at the different temperatures investigated. The difference between the aqueous domain higher and lower n values (Δn), 1 day after the shaking, is 1 order of magnitude larger than that reported in Figure 5 and the n gradient extends approximately over a region 2 mm thick, below the o–m interface. During the following days this region extends more and more and the Δn becomes smaller and smaller as well. Correspondingly a light intensity difference, 1 order of magnitude larger than for the stable sample, is measured 1 day after the shaking and progressively decreases during the following days. These results agree with the visual observation on the unstable sample which is composed of a high-turbidity intermediate region plus two practically transparent lower and upper regions, the diffuse region being more sharp than the stable sample. After one week, both $n(h)$ and $I(h)$ no longer seem to evolve. From an experimental point of view we decided that the sample was "stable" when we were not able to detect variations in the measurements during three weeks. In Figure 6c, the important index of refraction gradient in the subinterface region can be indeed representative of an incompletely stabilized sample.

The stabilization kinetics has also been tested by QELS, by measurements of the intensity correlation function, 1 mm below the o–m interface (for $\theta = 90°$), during all the stabilization time. At the beginning, the correlation function is not single exponential but is a superposition of exponential decays with time constants covering more than one decade and is higher than for the stable sample; this superposition is attributed to the fact that the unstable sample is likely a polydisperse emulsion. During a time comparable with the stabilization time previously defined, the intensity correlation function slowly becomes single exponential; thus the sample can be considered as monodisperse, within the sensitivity limits of the QELS detection. After 1 week (again for the following 3 weeks), no further evolution of the correlation time has been detected.

Discussion

The visual observation, performed to study the low surfactant concentration part of the phase diagram of the brine/toluene/1-butanol/SDS system, reveals a new behavior whose main characteristic is the coexistence of transparent oily regions with aqueous domains having a scattering power varying with the distance from the interface, h. The composition and structure measurements on a typical sample, within the temperature range where the peculiar behavior is observed, lead to better insight into the phenomenon. The upper region is confirmed to be a homogeneous oily solution similar to the excess oily phase of Winsor I and III microemulsions; it is mainly composed of toluene and 1-butanol. A correlation time of the scattered intensity is detected throughout the aqueous domain, implying that this whole domain is of microemulsion type. The $D(h)$ profile, detected for $\theta = 90°$, at $T = 20$ °C, clearly establishes the existence of two regions of constant D value corresponding to what we have called the intermediate and lower regions. They are separated by a region of rapidly varying D corresponding to the diffuse region.

Because the diffuse samples relax very slowly after a mechanical agitation and are placed on the phase boundaries between two- and three-phase coexistence regions, a possible explanation of the diffuseness can be an incomplete phase separation between the intermediate and the lower regions. However, at the end of the Results section, we have shown that, before attaining what we considered a "stable state", the aqueous domain is probably a polydisperse emulsion, the concentration gradients being larger than for the stable sample; thus under the hypothesis of a very slow equilibrium attainment we expect, as final state, a Winsor I equilibrium. The fact that the Winsor I equilibrium was never observed could simply signify that we did not wait the time necessary to observe it, time which could be of the order of months. Another possible explanation suggested by the dishomogeneity of the aqueous domain and by its important scattering power could be the proximity to a critical point. Moreover, we cannot exclude that the sample diffuseness is linked to a segregation due to gravity of dispersed objects having different sizes, whose formation could be favored by the peculiar composition of the studied microemulsion. The three possible explanations pointed out here have to be discussed on the basis of the experimental results.

In the limit of resolution of the QELS measurements, following the Kawasaki description, we can discuss the criticality of the phenomenon studying the τ^{-1}/q^2 dependence as a function of q^2.[26] This dependence is reported in Figure 7 for three different regions of the aqueous domain. As expected for a critical system, an increase of the function with q^2 is indeed observed; however, an interpretation of that variation in terms of a transition from homodyne to heterodyne detection seems more likely than in terms of critical behavior. In fact such a critical behavior should appear independently of h, while the observed variations depend on h (curve a is evidently not critical), and is not compatible with the observed saturation of all the curves at large q. Even if a critical behavior can be easily excluded, a precritical behavior could exist. It should be characterized by a linear dependence of τ^{-1}/q^2 vs. q^2.[27] On the basis of our experimental accuracy at large q, we can only say that the correction term, if it exists, is smaller than 6% and is hardly detectable; the same thing can be said at the higher temperature studied ($T = 23.78$ °C). In conclusion, a precritical regime cannot be excluded but it seems very unlikely because the temperature increase does not favor the transition toward a critical regime and correspondingly the sample diffuseness decreases as shown by the $I(t)$ curves and by the visual observation.

Supposing now that we interpret the correlation time, measured all throughout the aqueous domain, in terms of mutual diffusion coefficient of an oil-in-water microemulsion system varying with the height, one expects a volume fraction variation vs. the height, $\phi(h)$, and thus a $D(h)$ variation. Because the volume fraction variation of the dispersed phase is finite and small (due to the nature of the sample, no dilution procedure is utilizable to extrapolate the results toward $\phi \rightarrow 0$), a second virial correction in the $D(\phi)$ formula[28-30] must be considered. In order to evaluate such a correction, we can first calculate the average volume fraction of the dispersed phase, ϕ (using the average composition of the aqueous domain at $T = 20$ °C reported in Table II), and four additional hypotheses: (i) all the surfactant molecules are aggregated (the quantity of surfactant molecules absorbed at the o–m interface and on the cell walls is negligible supposing a monolayer adsorption); (ii) the whole toluene content of the aqueous domain belongs to the dispersed phase; (iii) the continuous phase contains the same 1-butanol content (0.02 mL) as the S0 sample lower phase (the 1-butanol partition coefficient between the continuous and the dispersed phases estimated from titration curves[7] confirms the validity of this hypothesis); (iv) we attribute to the dispersed phase the n value of toluene. The evaluated average volume fraction results in $\phi = 0.0275$ at $T = 20$ °C. Dividing now the overall aqueous domain into slices of about constant n, we can deduce a volume fraction profile $\phi(h)$. The values obtained for the intermediate and lower regions are respectively 0.0274 and 0.0260. Taking as an upper limit of the virial coefficient absolute value, $\alpha = 20$ (one of the larger values found in the literature[29]) and the previously calculated $\Delta\phi$, the corresponding expected D variation is only of 3%. If the globules radius (R_H) is kept constant we cannot interpret the 50% measured D variation between the lower and intermediate regions, in terms of volume fraction variation at constant size. Thus the $D(h)$ profile rather suggests the existence of two neighboring regions with scattering objects of different size. Assuming that globules are

(26) Berge, P.; Calmette, P.; Laj, C.; Tournaire, M.; Volochine, B. *Phys. Rev. Lett.* **1970**, *24*(22), 1223.
(27) Fourche, G.; Bellocq, A. M.; Brunetti, S. *J. Colloid Interface Sci.* **1982**, *88*, 307.
(28) Corti, M.; Degiorgio, V. *J. Phys. Chem.* **1981**, *85*, 711.
(29) Cazabat, A. M.; Langevin, D. *J. Chem. Phys.* **1982**, *74*(6), 3148.
(30) Bellocq, A. M.; Biais, J.; Bothorel, P.; Clin, B.; Fourche, G.; Lalanne, P.; Lemaire, B.; Lemanceau, B.; Roux, D. *Adv. Colloid Interface Sci.* **1984**, *20*, 167.

dispersed throughout the aqueous domain, the average radius of the globules (R) can be evaluated as a function of ϕ, $R = 3\phi/(n_s\Sigma)$, where n_s is the number of surfactant molecules per unit volume and Σ is the area per surfactant molecule of the interfacial film ($\Sigma \simeq 60$ Å^2).[31] Usually the Σ value is related to one surfactant molecule plus one alcohol molecule; however, in the present case we do not know the composition of the interfacial film. In order to do a reasonable estimation of R, the average composition of the dispersed phase into the aqueous domain (toluene 0.0234 mL, 1-butanol 0.0048 mL, and SDS 5.81×10^{-4} mL) can be used. Moreover, supposing that the 1-butanol/toluene ratio of the upper phase is maintained into the droplet core of the dispersed phase, the 1-butanol content adsorbed at the interface results $4.32 \times 10^{-5}N_A$ molecules (N_A, Avogadro number) and the total SDS content at the interface, $2.34 \times 10^{-6}N_A$ molecules. The above evaluation leads to an interfacial 1-butanol/SDS ratio $\sim$ 20 much larger than usual. Such a result can be an important characteristic of that low SDS content system. It means that the interfacial alcohol has to be included in the estimation of n_s; thus attributing a 60 Å^2 area to 2 or 3 interfacial molecules (SDS or alcohol), we get $R \sim 100$–150 Å. From the mutual diffusion coefficient we can also give a rough estimate of a hydrodynamic radius R_H, neglecting corrections due to the finite concentration of the sample but simply using the Stokes–Einstein formula[11] (namely assuming $D \sim D_0$); assuming as viscosity that of water we get $R_H \sim 200$ Å, in qualitative good agreement with the R value deduced from the composition analysis. Moreover, we obtain $R_H = 230$ and 160 Å in the intermediate and lower regions, respectively. These values are surely overestimated as the second virial coefficient contribution has been neglected, but the ratio between them ($\sim$1.5) is presumably correct because of the small $\phi(h)$ variation between the two regions. The description of the aqueous domain in terms of a uniform continuous phase and two dispersed phases characterized by different globule sizes seems reasonable. These two dispersed phases appear spatially separated (different h zones) but the transition between them is progressive. The $I(h)$ profiles give a support to that interpretation. Indeed a factor 1.5 on the radius of the droplets implies a factor of 3–4 on the scattered intensity, i.e., the same factor on the difference between transmitted intensity and incident light intensity. We have no measurements in the very bottom of the cell; anyhow the trend of the $I(h)$ profile is clear: larger scattering close to the o–m interface.

Under the hypothesis of globules of different size coexisting within an identical continous medium, the question is now to try to understand the origin of their spatial separation. First the interactions between globules are likely attractive and may favor the formation of aggregates (dimers, trimers, ...).[32-37] On the other hand, we have seen that a plausible analysis of the compositions leads to a rather high alcohol content in the interfacial film (compared to conventional microemulsions). Usually, an increase of the alcohol content in the interfacial film leads to a decrease of the elastic coefficient K associated with the film curvature.[38] If C_0 is the spontaneous curvature of the film, the energy necessary to get a curvature $C \neq C_0$ is $E = (1/2)K(C - C_0)^2$. Low K values can lead to large polydispersity by thermal fluctuations.[39-41] If several sizes coexist either by aggregation or curvature fluctuation, in both cases, a sedimentation of the large enough globules may arise due to gravity. The competition between Brownian motion and gravity gives an exponential distribution $\exp(-\Delta\rho Vgh/k_BT)$ with $\Delta\rho$ the density difference between the continuous and the dispersed phase, V the droplet volume, and g acceleration due to gravity. The characteristic length scale over which sedimentation occurs is $l = k_BT/\Delta\rho Vg$. With $\Delta\rho = 0.13$ g/cm^3, we get $l = 18$ cm for $R = 160$ Å, and $l = 6$ cm for $R = 230$ Å. If the system is polydisperse enough, the size distribution should thus vary with h, larger globules sedimenting toward the oil–microemulsion interface. Of course a sum of two exponential decays should give a monotonic decreasing function; the constancy of the profiles in the sample intermediate region suggests that a gravity segregation alone cannot explain the whole trend of the profiles. We have tried to detect an eventual polydispersity variation with h in the QELS experiments, looking for a long time tail in the correlation function or systematic h dependences in the quality of fit, without obtaining a clear answer. It is a classical but delicate question: for example, a 10% amount of aggregates of two droplets in the dispersion is hardly detectable: the correlation times are not separated enough to give visible distortion of the correlation function, especially at large scattering angle, as the larger aggregates scatter more strongly in the forward direction. We have indeed observed that the quality of fit was slightly worse for small-angle scattering in the intermediate region, but this effect can as well be attributed to a partial transition to a heterodyne detection. A clearly detectable polydispersity was observed only for unstable samples as reported at the end of the Results section.

We have to discuss now the high sensitivity of the system to the temperature which may arise from two effects: (1) the strength of the interactions is certainly temperature dependent; (2) the rigidity coefficient of the layers (K) is also strongly sensitive to temperature. It is unfortunately not possible to characterize in more detail the temperature and concentration dependences of the interactions in that system as dilution procedures are obviously not usable. On the other hand it would be quite important to directly measure the rigidity modulus of the interfacial film K, using, for example, EPR techniques,[42] in order to see if this is effectively the leading term controlling the phase equilibrium of the system studied, as in Winsor equilibria. At the present state of the research, we recall that for $T = 12$ °C, the surfactant was adsorbed on the o–m interface and on the cell walls as white platelets. This may correspond to a film transition toward lamellar structures close to 12 °C, indicating a rigidity coefficient $K > K_BT$[38] at that temperature. With increasing temperature, a K_BT value higher than K favors the appearance of a microemulsion in the whole aqueous domain as observed ($T = 30$ °C series of the phase diagram of Figure 3) and as deduced by the trends of the $I(h)$ and $n(h)$ profiles at $T = 24$ °C, shown on Figures 5 and 6. For intermediate temperatures an intermediate case can be expected: the competition between rigidity and thermal energy could favor the coexistence between globules and dimeric aggregates (curvatures of opposite sign give a low average curvature value of the aggregate) or simply the coexistence of globules of different size. To clear this point, a structural investigation of the anisotropic state of the sample must be done.

Conclusion

From an analysis of the phase diagram of the brine/toluene/1-butanol/SDS system in the low surfactant concentration region we have pointed out the existence of a zone in which a new behavior, characterized by the presence of an aqueous domain with composition and structure progressively varying with height, has been detected. This aqueous domain coexists with more conventional regions (oily or microemulsions). Detailed composition and structural investigations on a typical sample, performed mainly by index of refraction, turbidity, and QELS measurements, in the temperature range where the diffuseness exists, have allowed us to establish that the upper region is an excess oily region, while

(31) de Gennes, P. G.; Taupin, C. *J. Phys. Chem.* **1982**, *86*, 2294.
(32) Ober, R.; Taupin, C. *J. Phys. Chem.* **1980**, *84*, 2418.
(33) Bellocq, A. M.; Bourbon, D.; Lemanceau, B.; Fourche, G. *J. Colloid Interface Sci.*, **1982**, *89*, 427.
(34) Guering, P.; Cazabat, A. M. *J. Phys. Lett.* **1983**, *44*, L-601.
(35) Safran, S. A.; Turkevich, L. A. *Phys. Rev. Lett.* **1983**, *50*, 1930.
(36) Safran, S. A. *J. Chem. Phys.* **1983**, *78(4)*, 2073.
(37) Huang, J. S.; Safran, S. A.; Kim, M. N.; Grest, G. S.; Kotlarchyk, M.; Quirke, N. *Phys. Rev. Lett* **1984**, *53(6)*, 592.
(38) Auvray, L. *J. Phys. Lett.* **1985**, *46*, L-163.
(39) Ruckenstein, E. In *Surfactants in Solution*; Mittal, K. L., Lindman, B., Eds.; Plenum: New York, 1984; Vol. 3, p 1551.
(40) Safran, S. A. In *Statistical Thermodynamics of Micelles and Microemulsions*; Chen, S. H., Ed.; Springer-Verlag: West Berlin, in press.
(41) Good, R. J.; Van Oss, C. J.; Broers, G. E.; Yang, X. *J. Colloid Interface Sci.* **1986**, *110(2)*, 604.
(42) Di Meglio, J. M.; Dvolaitzsky, M.; Ober, R.; Taupin, C. *J. Phys. Lett.* **1983**, *44*, L-229. *J. Phys. Chem.* **1984**, *88*, 6036.

the aqueous domain is of the o/w microemulsion type, down to the bottom of the cell. Although the description of the sample composition and structure (within the thermal range where the diffuseness is observed) is rather satisfactory, the main questions about the nature and the origin of the diffuseness are not fully answered. In fact the new behavior cannot be attributed without doubt to thermodynamically stable samples but it could be as well a stage of a very slow evolution toward a final state of Winsor I type. Whether thermodynamically stable or not, the samples studied present some interesting characteristics. It is demonstrated that a microemulsion is obtained down to a very low surfactant content. The fact that the studied state could be unstable does not change this conclusion because the trend of the evolution is clearly toward a homogeneous o/w microemulsion in equilibrium with an excess oily phase, if an evolution exists. The microemulsion interfacial film appears to be very rich in alcohol, presenting an alcohol/surfactant ratio 1 order of magnitude larger than for usual Winsor phases. Such a film rich in alcohol is expected to present peculiar mechanical characteristics corresponding to a quite low rigidity coefficient of the interface: the proximity in temperature of the zone in which the new behavior is observed to the solubilization limit of the surfactant and the high sensitivity of the sample to temperature changes. The diffuseness of the samples seems not linked to a critical state but more likely to the coexistence of globules differing in size. At the present state of the measurements we have no information on the shape of the globules. The 1.5 ratio between the diameters of the globules of the intermediate and lower regions could support the hypothesis of an intermediate region mainly composed of oily dimeric aggregates. Moreover, the particular composition of the interfacial film could favor strong curvature fluctuations leading to polydispersity or aggregation.

Acknowledgment. We thank D. Ausserrê, L. Auvray, J. M. Di Meglio, M. Dvolaitzky, G. Guillot, H. Hervet, J. F. Joanny, and R. Ober for very helpful discussions and assistance in the experiments, and Dr. G. Menchi who made the gas chromatographic measurements. We thank Professor B. Widom and Professors C. M. Knobler and J. Wheeler for very stimulating discussions. C. G. is grateful to Prof. P. G. de Gennes for his kind hospitality and for helpful discussions and criticisms during the course of this work. She thanks the Italian Foundation "Angelo Della Riccia" and the Italian C.N.R. for financial support which made it possible for her to start in this work.

Registry No. SDS, 151-21-3; NaCl, 7647-14-5; toluene, 108-88-3; 1-butanol, 71-36-3.